EPS-0468
Submitted to Pa 14 and Pl 3,4,11

Photoproduction of J/ψ Mesons at HERA

H1 Collaboration

Abstract

Results on J/ψ production in ep interactions from the H1 experiment at HERA are presented. The data correspond to an integrated luminosity of $2.8\,\mathrm{pb}^{-1}$. The J/ψ mesons are produced in photoproduction ($Q^2 \rightarrow 0$) and detected via their leptonic decays. The γp cross section for elastic J/ψ production is observed to increase strongly with the center-of-mass energy. The γp cross section for inelastic J/ψ production is compared to NLO QCD-calculations in a colour singlet model. Agreement in shape is found if for the proton a gluon distribution rising towards low x is used.

1. Introduction

Two distinct types of models have been used to describe photoproduction of J/ψ mesons. A diffractive mechanism (Pomeron exchange)[1] can be used to describe elastic J/ψ production (fig. 1a) and also events with proton dissociation (fig. 1b).
Recently attempts were made to replace the pomeron by a gluon-ladder within a QCD model [2].
In perturbative QCD inelastic J/ψ production can be described as a Photon Gluon Fusion process in the colour singlet model [3] (fig. 1c). Recently NLO calculations have been performed for this process [4].

2. Experimental Setup

At HERA 820 GeV protons collide with 27.6 GeV positrons resulting in a center of mass energy of $\sqrt{s} = 300$ GeV. The main components of the H1 detector [6] used in the present analysis are the tracking system, consisting of the forward- and central-drift chambers, and the electromagnetic and hadronic part of the liquid argon (LAr) calorimeter. These components are mounted concentrically around the beamline inside a homogenous magnetic field of 1.15 T. The instrumented iron yoke surrounding the detector is used for muon detection.

3. Trigger and Event Selection

Events are selected where the scattered positron is not observed in the detector which corresponds to $Q^2 < 4\,\mathrm{GeV}^2$. The J/ψ mesons are identified by their decays into lepton pairs (electrons or muons). Electrons are detected in the electromagnetic part of the LAr-calorimeter by linking a drift-chamber track to a calorimeter cluster and demanding the measured energy to be comparable to the momentum.
Drift-chamber tracks are identified as muons if they are either linked to track elements reconstructed in the muon detector or if they are identified as minimum ionizing particles in the LAr-Calorimeter.
A lepton pair candidate is defined by two drift-chamber tracks with opposite charge in the range of polar angles $20° \leq \theta \leq 160°$ with momenta above 0.8 GeV which are identified as leptons. Both drift-chamber tracks have to be fitted to the reconstructed primary event vertex.
J/ψ events are triggered either by topology triggers based on the tracking system or by triggers which are sensitive to at least one lepton in the LAr-Calorimeter or the instrumented iron combined with the tracking system.
The mass distributions for elastic e^+e^- pairs and for elastic and inelastic $\mu^+\mu^-$ pairs are shown in fig. 2. The separation between elastic and inelastic events is defined below. Clear signals are observed at the J/ψ mass. Lepton pairs with an invariant mass in a region of ± 225 MeV around the nominal J/ψ mass are called J/ψ candidates. While the background in the case of elastic J/ψ production is described by a two photon process (QED), the background in the inelastic channel is due to muons from the semileptonic decay of hadrons and to misidentified pions. The background was estimated by fitting a Gaussian plus a linear function and was subtracted.

The inelasticity z is the main parameter for the separation of elastic and inelastic J/ψ candidates. It is defined as $z = \frac{P_p \cdot P_\psi}{P_p \cdot P_\gamma}$, where P_p, P_ψ and P_γ are the 4-vectors of the incoming proton, the J/ψ and the exchanged photon (P_γ is determined using the Jaquet-Blondel method). In fig. 3 the z distribution for all measured J/ψ-candidates in the muon channel is shown in comparison with Monte Carlo predictions.

Events are classified as inelastic in the z-range $0.45 \leq z \leq 0.9$. Below $z < 0.45$ resolved photon processes are expected to contribute. The contamination in the selected sample is below 7% as estimated by a Monte Carlo calculation [10].
Events are classified as elastic in the range $z > 0.95$ if there are exactly 2 tracks and if no further activity in the forward part of the detector is seen. This veto against hadronic activity in the very forward region of the detector is based on the low θ-part ($\leq 10°$) of the LAr-Calorimeter, the forward muon system ($3° \leq \theta \leq 17°$) and the proton tagging system ($\theta \leq 0.06°$), an array of scintillators placed 24 m from the interaction point in the direction of the proton.

4. Acceptance

The geometrical acceptance for J/ψ meson production if both leptons are required to be within the acceptance region $20° \leq \theta \leq 160°$ is calculated for $Q^2 \leq 4\,\mathrm{GeV}^2$ and $30\,\mathrm{GeV} \leq W_{\gamma p} \leq 180\,\mathrm{GeV}$ for muons and $30\,\mathrm{GeV} \leq W_{\gamma p} \leq 150\,\mathrm{GeV}$ for electrons. For elastic J/ψ-production the acceptance is given in table 1. For inelastic production the acceptance for the muon channel is found to be $(62 \pm 4)\%$.

5. Elastic J/ψ production

The efficiencies and cross sections for elastic J/ψ production are given in table 1. The analysis efficiency contains efficiencies for track reconstruction in the driftchambers, muon identification, and additional selection cuts. The systematic errors for the efficiencies (analysis and trigger) are estimated by a comparison of data and Monte Carlo simulation. The elastic cross-sections are corrected for a contamination of $(21 \pm 5)\%$ proton dissociation. The contamination is determined in a model independent way using the forward detectors. The experimentally determined fraction of proton dissociated events agrees well with a Monte Carlo simulation, where 50 % proton dissociation is assumed. The ep-cross section is converted to a γp-cross section using the photon flux which is calculated to be 0.160 in the interval of $30\,\mathrm{GeV} \leq W_{\gamma p} \leq 180\,\mathrm{GeV}$ and 0.146 within $30\,\mathrm{GeV} \leq W_{\gamma p} \leq 150\,\mathrm{GeV}$.

The γp-cross section for elastic J/ψ production measured via the electron and muon decays is presented in fig. 4 in comparison with measurements by the ZEUS collaboration [7] and fixed target experiments [8, 9].

6. Inelastic J/ψ production

The inelastic J/ψ cross section for $z \leq 0.9$ was obtained in a similar way. Events with $0.45 \leq z \leq 0.9$ were used and a correction of 11% determined by Monte Carlo [10] for the contribution of $z \leq 0.45$ was applied. The differential cross-section $\sigma(\gamma p \rightarrow J/\psi X)$ as a

analysis channel	$J/\psi \to \mu^+\mu^-$	$J/\psi \to e^+e^-$
analysis efficiency	0.47± 0.05	0.48± 0.05
trigger efficiency	0.51± 0.06	0.46± 0.06
acceptance	0.56± 0.04	0.66± 0.03
$W_{\gamma p}$[GeV]	[30, 180]	[30, 150]
branching ratio	0.060±0.003	
#events	216± 17	147± 13
$\int Ldt$[nb^{-1}]	2843± 85	2098±70
ep-cross-section[nb]	9.4± 1.35	8.0± 1.38
γp-cross-section[nb]	58.8 ± 8.4	54.5 ± 10.3

Table 1: Efficiencies and cross sections for elastic J/ψ production (preliminary). The errors contain statistical and systematic errors added in quadrature.

function of $W_{\gamma p}$ is shown in fig. 5. It is compared to NLO-calculations with different gluon density functions and for different values of the charm mass m_c and the strong coupling constant α_s [4].
The data are above the predicted cross sections by at least a factor two. The prediction that comes closest to the data uses a gluon density rising at low x_{gluon} (MRS(G)), a light charm quark mass (1.4 GeV), and a value of $\alpha_s = 0.30$.
The analysis was repeated demanding a higher inelasticity $z < 0.8$ and in addition a $p_T(J/\psi) > 1$ GeV. These cuts were proposed to stay clear of regions where the NLO calculations are problematic [12]. The comparison with the calculations is shown in fig. 6. Agreement within errors is observed.

7. Conclusion

At center-of-mass energies of about 100 GeV elastic J/ψ production at $Q^2 \approx 0$ shows an increase with $W_{\gamma p}$ which can be parameterised by $W_{\gamma p}^{4\epsilon}$, $\epsilon = 0.25$. The flat increase observed in hadroproduction does not describe the data.
The cross-section for inelastic J/ψ production is almost a factor 2 larger than predicted by the colour singlet model including NLO corrections. The measured $W_{\gamma p}$ dependence is compatible with the calculation using a gluon distribution in the proton increasing towards low x_{gluon}, such as in the MRS(G) parametrisation which also describes other HERA measurements, e.g. F_2 at low x.
Agreement within errors is obtained applying tighter cuts on inelasticity and p_T of the J/ψ.

Acknowledgements

We are very grateful to the HERA machine group whose outstanding efforts made this experiment possible. We acknowledge the support of the DESY technical staff. We appreciate the big effort of the engineers and technicians who constructed and maintained the detector. We thank the funding agencies for financial support of this experiment. We wish to thank the DESY directorate for the support and hospitality extended to the non–DESY members of the collaboration.

References

[1] G.A. Schuler and J. Terron, DESY-92-017 and CERN-TH-6403/92 (1992)

[2] M.G. Ryskin, Z. Phys. C57 (1993) 89

[3] E. L. Berger and D. Jones, Phys. Rev. D23 (1981) 1521

[4] M. Kraemer, J. Zunft, J. Steegborn and P.M. Zerwas, Phys. Lett. B348 (1995) 657

[5] H. Jung, G.A. Schuler and J. Terron, Int. Journ. Mod. Phys. A32 (1992) 7955

[6] H1 Collaboration, I. Abt et al., DESY-93-103 (1993)

[7] ZEUS Collaboration, M. Derrick et al., Phys. Lett. B350 (1995) 120

[8] E401 Collaboration, M. Binkley et al., Phys. Rev. Lett. 48 (1982) 73

[9] FTPS Collaboration, B. H. Denby et al., Phys. Rev. Lett. 52 (1984) 795

[10] H.Jung,Physics at HERA, Proc. of the workshop (1991) 1488

[11] B. List, Diploma Thesis (Tech. Univ. Berlin), 1993 (H1-NOTE 93-319)

[12] M. Kraemer, private communication

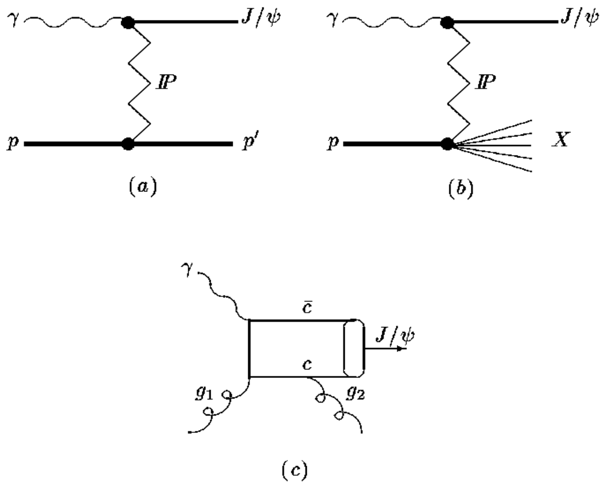

Figure 1: J/ψ production mechanism: (a) Elastic J/ψ production via pomeron exchange [1]; (b) Diffractive proton dissociation; (c) Photon Gluon Fusion model for inelastic J/ψ production [5]

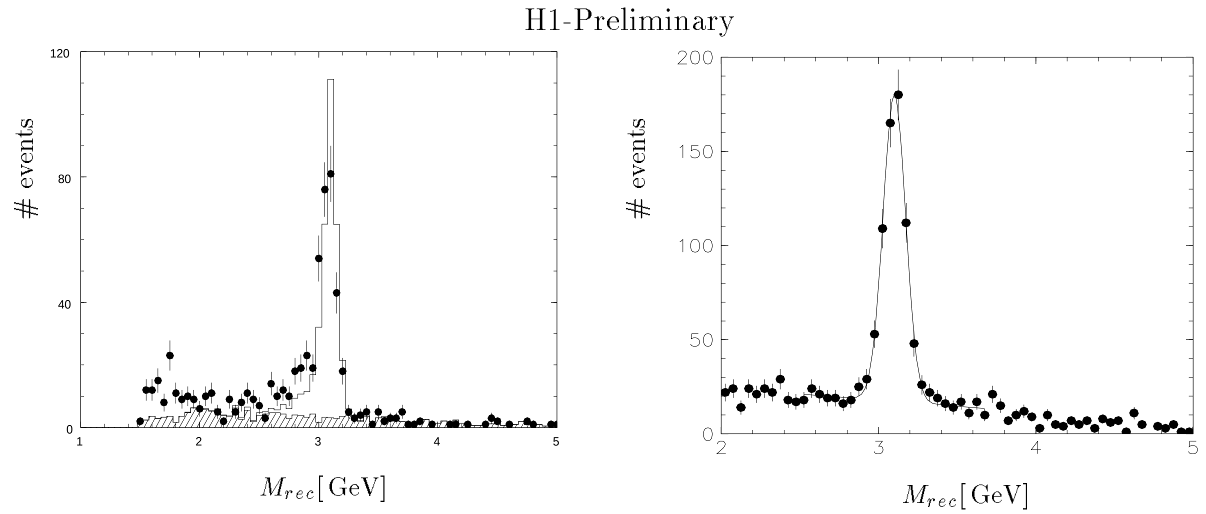

Figure 2: Left: Mass distribution of selected e^+e^- pairs for the elastic J/ψ sample. The data points are compared with Monte Carlo predictions. The hatched histogram shows the contribution of QED electron pairs. Right: Mass distribution of $\mu^+\mu^-$ pairs selected for elastic and inelastic J/ψ production . The data points are fitted by a Gaussian plus a linear background.

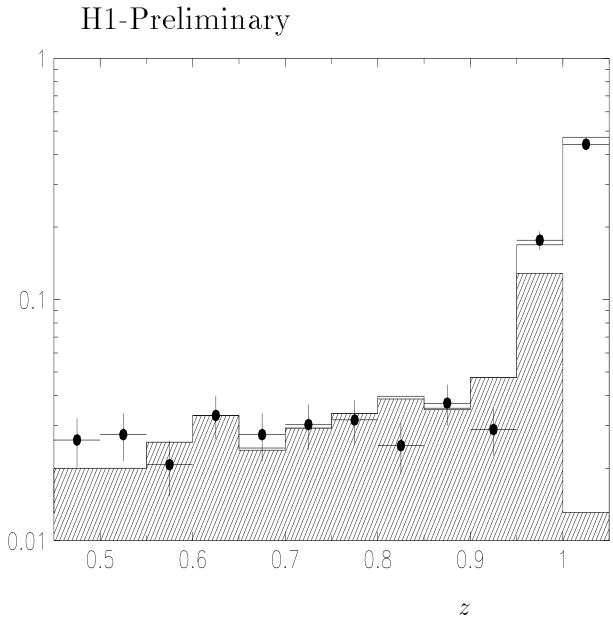

Figure 3: z distribution for all $J/\psi \rightarrow \mu^+\mu^-$ candidates. The shaded histogram shows a Boson-Gluon-Fusion Monte Carlo prediction (EPJPSI) [10], the histogram combines the Boson Gluon Fusion with a diffractive elastic Monte Carlo (DIFFVM) [11].

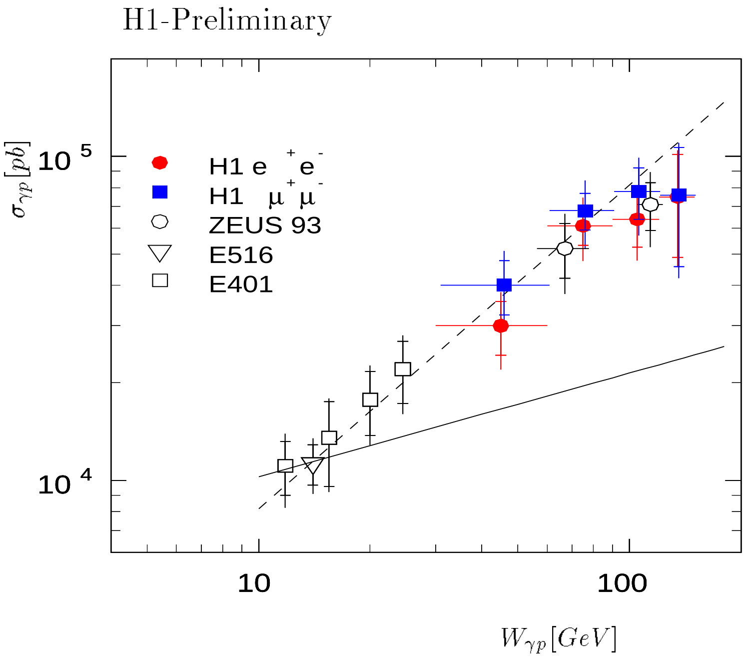

Figure 4: γp-cross section for elastic J/ψ production. The full line shows $\sigma_{\gamma p} \sim W_{\gamma p}^{4\epsilon}$ with $\epsilon = 0.081$ as predicted for soft pomeron exchange, the dashed line shows the same with $\epsilon = 0.25$. Both curves are normalized to the E516 data point. The outer (inner) error bars are the total (statistical) errors.

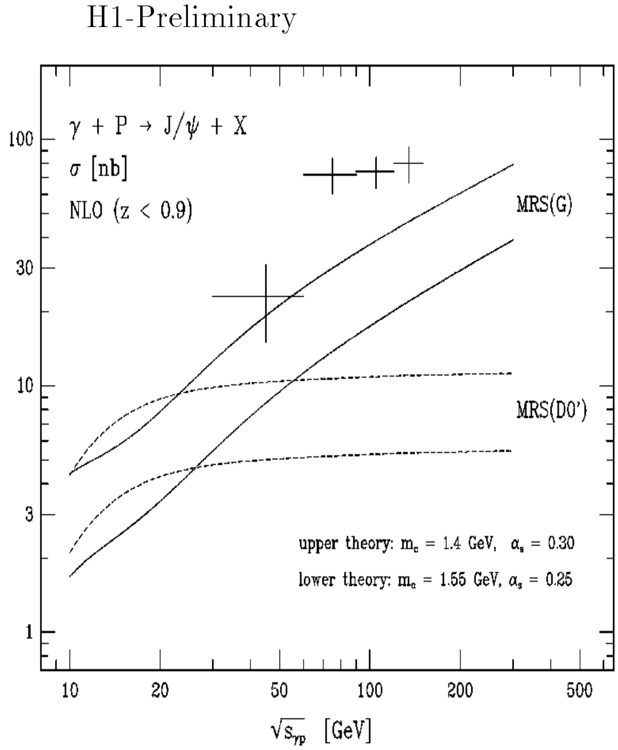

Figure 5: γp-cross section for inelastic J/ψ production. The theoretical curves are NLO calculations for different structure functions. The errors contain statistical and systematic ($\approx 20\%$) errors added in quadrature.

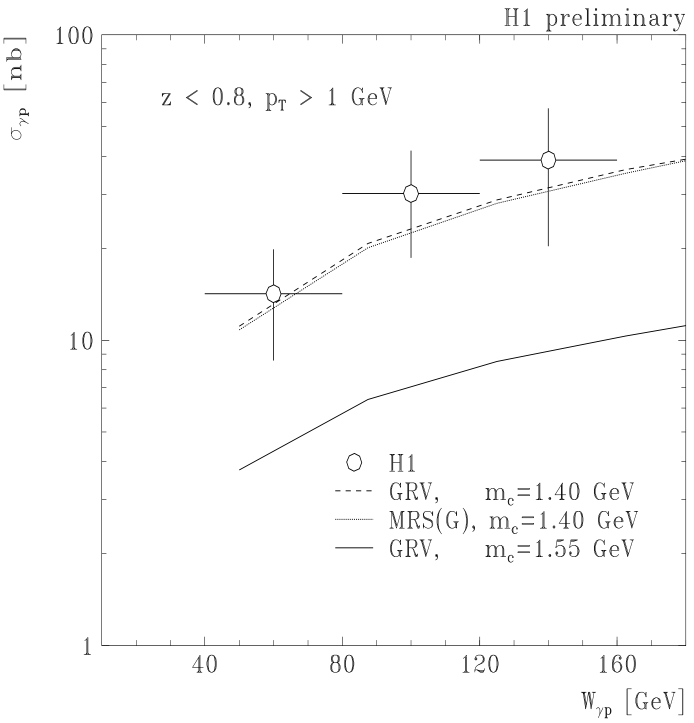

Figure 6: γp-cross section for inelastic J/ψ production in a restricted kinematical range.. The theoretical curves are NLO calculations for different structure functions. The errors contain statistical and systematic ($\approx 20\%$) errors added in quadrature.